Check for updates

# Preparation of novel chiral stationary phases based on a chiral trianglsalen macrocycle by thiol-ene click chemistry for enantioseparation in high-performance liquid chromatography†

Jia-Lei Wu, Hua-Can Zhang, Li-Qin Yu, Sheng-Ming Xie, [ID] Jun-Hui Zhang, [ID] * Bang-Jin Wang [ID] * and Li-Ming Yuan [ID] *

Macrocyclic compounds, with unique cyclic structures, well-defined molecular cavities and diverse functional properties, have shown broad application prospects in the fields of molecular recognition, catalysis, separation, and supramolecular chemistry. In this study, a novel chiral trianglsalen macrocycle (CTSM) was synthesized by a one-step condensation reaction of 3,3′-dihydroxy-(1,1′-biphenyl)-4,4′-dicarboxaldehyde with (1R,2R)-1,2-diaminocyclohexane. Then, the CTSM was bonded to thiol-functionalized silica by a thiol–ene click approach to prepare two chiral stationary phases (CSPs), CSP-A and CSP-B, with different spacers for high-performance liquid chromatography (HPLC). The two prepared CSPs exhibit excellent chiral separation performance, and 22 racemates were enantioseparated on these two CSPs, including alcohols, ketones, esters, phenols, organic acids, epoxides, and amines. Among them, 20 racemates achieved baseline separation on CSP-A, while 15 racemates achieved baseline separation on CSP-B. CSP-A shows better chiral separation capability than CSP-B, and most racemates obtain higher resolution ($R_s$) values because CSP-A features a cationic imidazolium spacer that enhances enantioseparation. Compared with commercial chiral columns (Chiralpak AD-H and Chiralcel OD-H), the prepared CSP-A shows peculiar advantages, achieving the separation of some enantiomers that cannot be separated or cannot be well separated by the two commercial columns. Furthermore, the effects of analyte mass, mobile phase composition, and column temperature on enantioseparation were studied. The two fabricated columns also exhibit good reproducibility and stability. After hundreds of uses of the columns, the relative standard deviations (RSDs, $n = 5$) for separations were less than 1.16% for the retention time and 3.29% for the $R_s$ value, respectively. Moreover, the RSDs ($n = 3$) of the $R_s$ value and retention time in terms of column-to-column reproducibility were less than 8.79% and 5.04%, respectively. This work demonstrates the promising potential of CTSM for chiral separation in HPLC.

# 1 Introduction

The efficient separation of chiral compounds is critically important in the fields of chemical synthesis, pharmaceutical production, agriculture, and food, due to the distinct toxicity and biological behaviors of enantiomers.[1–3] Among the current enantioseparation methods, high-performance liquid chromatography (HPLC) conducted on chiral stationary phases

(CSPs) has evolved into a highly efficient and versatile approach.[4–6] Meanwhile, the preparation of CSPs is considered to be the key to this approach. Thus, designing new CSPs with excellent enantiomeric recognition capabilities continues to be an area of active research. So far, a number of CSPs have been applied to HPLC chiral separation, including polysaccharides,[4,7] cyclodextrins,[8–10] crown ethers,[11,12] macrocyclic antibiotics,[13,14] and others.[15–20]

Macrocyclic compounds are a class of molecules with cyclic structures and well-defined internal molecular cavities, including crown ethers, cyclodextrins, cyclofructans, calix[n]arenes, cucurbit[n]urils, and pillar[n]arenes, which have come to be regarded as fundamental components of supramolecular chemistry.[21–24] Macrocyclic compounds, characterized by internal cavities, functional modifiability, and multiple synergistic interaction sites, demonstrate broad utility in molecular

*Yunnan Key Laboratory of Modern Separation Analysis and Substance Transformation, College of Chemistry and Chemical Engineering, Yunnan Normal University, Kunming 650500, P.R. China. E-mail: zjh19861202@126.com, wangbangjin711@163.com, yuan_limingpd@126.com*

recognition and separation,[25–28] catalysis,[29] and sensing.[30,31] In the field of chromatographic separation, macrocyclic compounds also hold a crucial position. For example, some macrocyclic compounds, such as crown ethers, cyclodextrins, cyclofructans, and macrocyclic antibiotics, have been successfully applied to the preparation of commercial chromatographic CSPs.[8–14,32,33] In recent years, some novel macrocyclic compounds have also been employed for chromatographic separation, achieving excellent separation performance.[34–38] Polyimine macrocycles (PMs), as a new class of macrocyclic compounds, are usually synthesized *via* the cycloimination of aldehydes with amines.[39,40] PMs are interconnected *via* rigid imine bonds to form a cyclic structure, thereby endowing the PM molecules with a more stable intramolecular cavity. Compared with other traditional macrocyclic compounds such as crown ethers, cucurbit[*n*]urils, and pillar[*n*]arenes, PMs exhibit some advantages. For example, PMs can be easily synthesized (the condensation of aldehydes with amines can achieve PMs in one step with high yield), and their molecular structure is more rigid, with a more stable cavity. The above advantages have attracted many fields of research on PMs, such as host-guest recognition and separation.[41–44] Trianglsalen macrocycles (TSMs) are a common type of PM with a shape similar to a triangle, which have attracted major attention in molecular recognition and separation.[41,42,45–47] However, there is still little research on the use of TSMs for HPLC separation.

In 2001, Sharpless first proposed "click" chemistry, a simple and efficient way for connecting reactants to obtain the desired products.[48] As a kind of click reaction, the "thiol-ene" click reaction is widely used in organic synthesis due to its high efficiency, mild reaction conditions, and broad application range. Because of its synthetic advantages, the "thiol-ene" click reaction is also one of the ideal methods for preparing chromatographic stationary phases by bonding selectors onto chromatographic matrices.[49–52]

Here, a chiral trianglsalen macrocycle (CTSM, $C_{60}H_{60}N_6O_6$) was synthesized by a one-step reaction of 3,3′-dihydroxy(1,1′-biphenyl)-4,4′-dicarboxaldehyde with chiral diamine (1*R*,2*R*)-1,2-diaminocyclohexane.[53] Then, two CSPs with different spacers were prepared by bonding the CTSM onto the thiol-functionalized silica *via* a thiol-ene click strategy. The chiral separation capabilities of the two CSPs were assessed, and the separation performance between the two CSPs and two commercially available columns (Chiralcel OD-H and Chiralpak AD-H) was compared. The effects of injected mass, mobile phase composition, and column temperature were discussed. Moreover, the reproducibility and stability of the two prepared columns were evaluated.

## 2 Experimental

### 2.1 Chemicals and reagents

3,3′-Dihydroxy(1,1′-biphenyl)-4,4′-dicarboxaldehyde, (1*R*,2*R*)-1,2-diaminocyclohexane, 1-allylimidazole, (3-mercaptopropyl)trimethoxysilane, 1,4-dibromobutane, 5-bromo-1-pentene, azo-

bisisobutyronitrile (AIBN), sodium hydride (NaH), and potassium carbonate ($K_2CO_3$) were obtained from Adamas-beta (Shanghai, China). Chloroform, tetrahydrofuran (THF), toluene, methanol (MeOH), ethanol (EtOH), acetonitrile (ACN), pyridine, acetone, hydrochloric acid (HCl), and magnesium sulfate ($MgSO_4$) were supplied by the Tianjin Fengchuan Fine Chemical Research Institute (Tianjin, China). HPLC-grade *n*-hexane (*n*-HEX) and isopropanol (IPA) were purchased from Sigma-Aldrich (Shanghai, China). Spherical silica gel (5 μm, 120 Å, 300 $m^2$ $g^{-1}$) was purchased from Nano-Micro Technology (Suzhou, China). Chiralpak AD-H (250 mm × 4.6 mm i.d.) and Chiralcel OD-H columns (250 mm × 4.6 mm i.d.) were purchased from Daicel Chiral Technologies (Shanghai, China). Detailed information about the tested racemates is provided in the ESI.†

### 2.2 Instrumentation

All chromatographic evaluations were performed on a Shimadzu LC-16 System (Japan), which was equipped with an SPD-16 UV-vis detector and a Lab Solutions LC workstation. The empty stainless steel HPLC column (250 mm × 2.1 mm i.d.) was packed using a slurry packer purchased from Alltech (USA). $^1H$ and $^{13}C$ nuclear magnetic resonance ($^1H$ NMR and $^{13}C$ NMR) spectra were recorded on a Bruker DRX-500 NMR spectrometer (Germany). Fourier transform infrared (FT-IR) spectra were determined using a Thermo Fisher Scientific Nicolet iS20 spectrometer (USA). Thermogravimetric analysis (TGA) was performed on an SDT-650 thermal analyzer (USA). Mass spectrometry data (ESI-MS) were obtained using a Thermo Scientific LTQ-Orbitrap XL electrospray ionization mass spectrometer (USA). Elemental analysis (EA) was performed on an Elementar Vario EL III analyzer (Germany).

### 2.3 Synthesis of chiral trianglsalen macrocycle (CTSM)

The synthesis of CTSM ($C_{60}H_{60}N_6O_6$) was performed according to the literature method (Fig. 1).[53] A solution of 3,3′-dihydroxy(1,1′-biphenyl)-4,4′-dicarboxaldehyde (121 mg, 0.5 mmol) in THF (25 mL) was prepared, followed by slow addition of an EtOH solution (25 mL) containing (1*R*,2*R*)-1,2-diaminocyclohexane (57 mg, 0.5 mmol). The reaction mixture was stirred at room temperature for 12 h. After solvent removal by rotary evaporation, the resulting solid was collected and repeatedly washed with EtOH. The product was obtained as a yellow solid after vacuum drying (120 mg, yield 75%). $^1H$ NMR (500 MHz, CDCl$_3$) δ 13.42 (s, 6H, OH), 8.29 (s, 6H, N=CH), 7.20 (d, 6H,
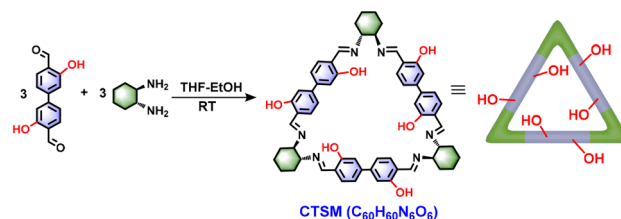


CTSM ($C_{60}H_{60}N_6O_6$)

**Fig. 1** Synthesis of CTSM.

ArH), 7.12 (s, 6H, ArH), 7.03 (d, 6H, ArH), 3.31–3.38 (m, 6H, CH–N), 1.48–2.01 (m, 24H, cyclohexyl CH$_2$). $^{13}$C NMR (125 MHz, CDCl$_3$) $\delta$ 164.41, 161.18, 144.20, 131.85, 118.10, 117.71, 115.46, 72.64, 33.18, 24.31 (see Fig. S1†).

### 2.4 Preparation of CSP-A and CSP-B

The two CSPs were prepared according to the route shown in Fig. 2. Initially, CTSM was functionalized with either 1,4-dibromobutane in combination with 1-allylimidazole or 5-bromo-1-pentene, yielding two modified products that contained C=C bonds. Subsequently, these products were bonded to thiol-functionalized silica *via* the thiol-ene click reaction, respectively, producing two CSPs (CSP-A and CSP-B) with different spacer groups. Detailed synthetic procedures are provided in the ESI.†

### 2.5 Column packing

The CSP (1.35 g) was dispersed in *n*-HEX/IPA (90/10, v/v, 30 mL) and ultrasonicated for 10 min to form a uniform suspension. Using *n*-HEX/IPA (90/10, v/v) as the propelling agent, the suspension was packed into an empty stainless steel column under 50 MPa for 30 min, followed by gradual depressurization. Column A was packed with CSP-A, while column B was packed with CSP-B. Subsequently, the packed columns were connected to the HPLC system and eluted with the mobile phase (*n*-HEX/IPA, 90/10, v/v) at a flow rate of 0.1 mL min$^{-1}$ for 3 h. The column efficiency of the fabricated columns was determined. The theoretical plate number measured with benzene was 18 500 plates per m for column A, and 17 200 plates per m for column B.

## 3 Results and discussion

### 3.1 Characterization of the CTSM and CSPs

The synthesized CTSM, CSP-A, and CSP-B were characterized by FT-IR, ESI-MS, NMR, TGA, and EA. The FT-IR spectrum of



**Fig. 2** (A) Preparation of CSP-A; and (B) preparation of CSP-B.

the CTSM (Fig. S2A†) showed a strong peak at 1624 cm$^{-1}$, corresponding to the characteristic absorption of the imine bond (–C=N–). Peaks at 1550 cm$^{-1}$, 1496 cm$^{-1}$, and 1446 cm$^{-1}$ were attributed to the benzene ring skeleton vibration, while those at 2928 cm$^{-1}$ and 2858 cm$^{-1}$ originated from saturated C–H stretching vibrations. The exact mass of CTSM (C$_{60}$H$_{60}$N$_6$O$_6$) was calculated to be 960.4574. The ESI-MS spectrum (Fig. S2B†) exhibited two prominent ion peaks at *m/z* = 961.4631 and 481.2321, consistent with the [M + H]$^+$ and [M + 2H]$^{2+}$ species of CTSM. Combined with $^1$H and $^{13}$C NMR (Fig. S1†), the successful synthesis of CTSM was further confirmed.

The comparative FT-IR spectra of CTSM, CSP-A, CSP-B, and SiO$_2$-SH are presented in Fig. 3A. Notably, the characteristic peaks of the two CSPs at 2928 cm$^{-1}$, 2858 cm$^{-1}$, and 1624 cm$^{-1}$ exhibit significant enhancement in comparison with SiO$_2$-SH due to the absorption of –CH$_2$, –CH–, and –C=N– groups in the bonded CTSM. Additionally, three new absorption bands emerged at 1550 cm$^{-1}$, 1496 cm$^{-1}$, and 1446 cm$^{-1}$ in the two CSPs, attributed to benzene ring skeletal vibrations of bonded CTSM. The characteristic peak changes of CSPs confirmed the success of the thiol-ene click reaction. TGA results (Fig. 3B) revealed pronounced weight loss for CSP-A and CSP-B compared to SiO$_2$-SH due to the decomposition of the organic components of the bonded CTSM. Besides, elemental analysis (Table S1†) demonstrated significantly increased C, N, and H contents in the two CSPs. These findings collectively verify the successful bonding of CTSM onto SiO$_2$-SH *via* thiol-ene click chemistry. Furthermore, the surface bonding amounts were computed to be 0.11 and 0.14 μmol m$^{-2}$ for CSP-A and CSP-B, respectively, as calculated using eqn (1) in the ESI.†

### 3.2 Resolution of racemates on CTSM-based CSPs

To evaluate the chiral separation performance of the CTSM-based CSPs (CSP-A and CSP-B), a variety of racemates (molecular structures presented in Fig. S3†), including alcohols, ketones, esters, phenols, organic acids, epoxides, and amines, were selected for separation on the two CSP packed columns (column A and column B). As summarized in Table 1 and Fig. S4,† both of the CSPs achieved successful enantiosepara-
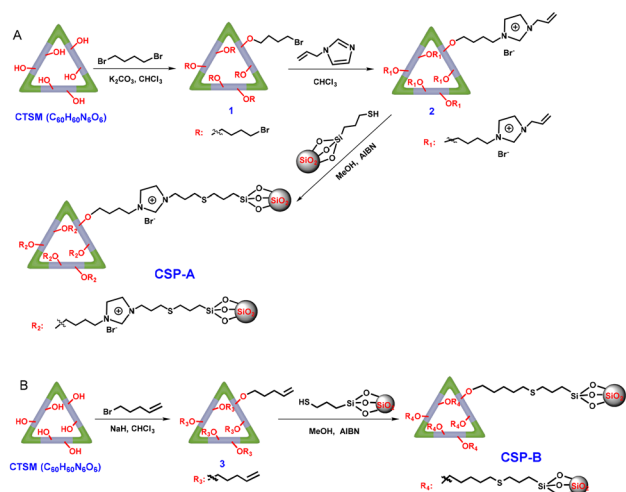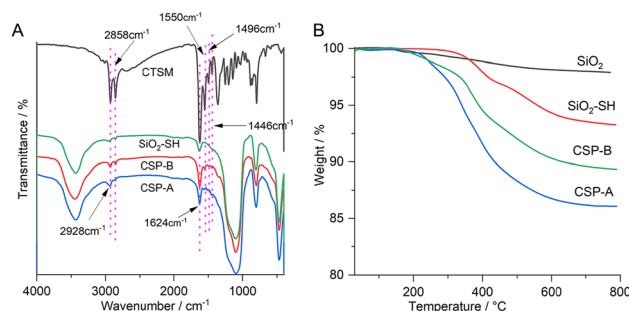


**Fig. 3** (A) FT-IR spectra of CTSM, SiO$_2$-SH, CSP-A, and CSP-B. (B) TGA curves of SiO$_2$, SiO$_2$-SH, CSP-A, and CSP-B.

**Table 1**  Enantioseparation data on column A, column B, the Chiralpak AD-H column, and the Chiralcel OD-H column

| Racemates | Column A (CSP-A) | | | Column B (CSP-B) | | | Chiralpak AD-H | | | Chiralcel OD-H | | |
|---|---|---|---|---|---|---|---|---|---|---|---|---|
| | $k_1$ | $\alpha$ | $R_s$ | $k_1$ | $\alpha$ | $R_s$ | $k_1$ | $\alpha$ | $R_s$ | $k_1$ | $\alpha$ | $R_s$ |
| 4,4′-Difluorobenzoin | 0.57 | 4.87 | 9.70 | 0.55 | 3.34 | 6.28 | 4.36 | 1.10 | 2.09 | 1.81 | 1.09 | 0.93 |
| 4,4′-Dimethylbenzoin | 0.47 | 4.01 | 8.73 | 0.53 | 3.01 | 4.56 | 5.06 | 1.10 | 2.74 | 1.69 | 1.36 | 2.39 |
| Methyl mandelate | 0.92 | 2.95 | 7.82 | 0.94 | 1.64 | 2.84 | 1.92 | 1.08 | 1.63 | 1.45 | 2.04 | 7.68 |
| 4-Chlorobenzhydrol | 0.45 | 4.66 | 7.48 | 0.70 | 1.83 | 2.79 | 1.65 | 1.14 | 2.01 | 2.05 | 1.00 | — |
| 4-Methylbenzhydrol | 0.54 | 3.07 | 7.11 | 0.70 | 1.56 | 2.17 | 1.66 | 1.11 | 1.66 | 1.74 | 1.13 | 1.46 |
| 1,1′-Bi-2-naphthol | 0.51 | 3.51 | 5.63 | 0.84 | 1.00 | — | 7.44 | 1.03 | 0.10 | 3.80 | 1.11 | 1.25 |
| 3-Hydroxy-2-butanone | 0.58 | 2.68 | 5.56 | 0.52 | 1.94 | 2.36 | 1.29 | 1.00 | — | 0.84 | 1.00 | — |
| Ethyl mandelate | 0.64 | 3.15 | 5.41 | 0.71 | 1.58 | 2.17 | 1.92 | 1.08 | 1.63 | 1.45 | 2.04 | 7.68 |
| 1-Phenylethanol | 0.54 | 2.13 | 4.48 | 0.62 | 1.13 | 0.54 | 0.84 | 1.00 | — | 0.90 | 1.22 | 1.29 |
| 1-Indanol | 1.04 | 2.22 | 4.32 | 0.84 | 1.00 | — | 1.23 | 1.07 | 1.17 | 0.97 | 1.16 | 1.08 |
| Ketoprofen | 0.56 | 2.47 | 4.28 | 0.54 | 1.50 | 1.44 | 1.08 | 1.37 | 3.67 | 2.99 | 1.00 | – |
| 2-Methoxy-2-phenylethanol | 0.53 | 2.11 | 4.22 | 0.66 | 1.33 | 1.46 | 0.91 | 1.23 | 2.70 | 0.81 | 1.13 | 0.69 |
| 1-Phenyl-1-pentanol | 0.26 | 2.56 | 3.70 | 0.31 | 1.47 | 1.07 | 0.78 | 1.00 | — | 0.74 | 1.00 | — |
| Benzoin | 0.54 | 1.85 | 3.18 | 0.62 | 1.91 | 2.85 | 4.45 | 1.34 | 6.35 | 1.53 | 1.41 | 2.85 |
| Mandelic acid | 0.43 | 2.05 | 3.09 | 0.56 | 1.56 | 1.97 | 2.95 | 1.19 | 2.30 | 1.67 | 1.29 | 2.14 |
| 2-Phenylcyclohexanone | 0.54 | 1.72 | 2.95 | 0.56 | 1.54 | 1.73 | 0.89 | 1.00 | — | 1.23 | 1.15 | 1.22 |
| 1-(4-Fluorophenyl)ethanol | 0.52 | 2.13 | 2.90 | 0.56 | 1.20 | 0.67 | 0.83 | 1.00 | — | 0.74 | 1.00 | — |
| 1-Phenyl-1-propanol | 0.43 | 2.22 | 2.58 | 0.44 | 1.28 | 0.90 | 0.83 | 1.11 | 0.50 | 0.83 | 1.06 | 0.63 |
| 2-Phenyl-1-propanol | 0.57 | 1.90 | 2.36 | 0.73 | 1.00 | — | 0.88 | 1.02 | 0.30 | 0.82 | 1.00 | — |
| 1-(4-Fluorophenyl)ethanamine | 0.32 | 1.69 | 2.29 | 0.32 | 1.76 | 1.62 | 0.86 | 1.00 | — | 0.92 | 1.13 | 0.96 |
| Styrene oxide | 0.44 | 1.29 | 1.22 | 0.39 | 1.62 | 1.65 | 0.41 | 1.10 | 0.67 | 0.64 | 1.00 | — |
| Amlodipine | 2.35 | 1.09 | 0.53 | 3.10 | 1.00 | — | 1.79 | 1.26 | 3.60 | 4.42 | 1.06 | 0.46 |
| 2,2,2-Trifluoro-1-(9-anthryl)ethanol | 0.38 | 1.00 | — | 0.54 | 2.30 | 3.69 | 1.76 | 1.52 | 3.30 | 1.97 | 3.10 | 11.1 |
| 3-(Benzyloxy)propane-1,2-diol | 4.76 | 1.00 | — | 2.50 | 1.64 | 3.64 | 2.24 | 1.19 | 0.70 | 2.73 | 1.06 | 2.12 |
| 1-Phenylethylamine | 0.29 | 1.00 | — | 0.35 | 1.77 | 1.80 | 0.71 | 1.00 | — | 0.96 | 1.19 | 0.81 |
| Flavanone | 0.74 | 1.00 | — | 1.00 | 1.20 | 0.90 | 1.45 | 1.07 | 1.16 | 1.55 | 1.42 | 3.66 |

HPLC conditions: column temperature: 25 °C; mobile phase: $n$-HEX/IPA = 90/10 (v/v); flow rate, 0.1 mL min$^{-1}$ for the fabricated columns, and 0.5 mL min$^{-1}$ for Chiralpak AD-H and Chiralcel OD-H; —: no separation.

tion for 22 chiral compounds, and the obtained chromatograms are shown in Fig. 4 and 5. As can be seen in Fig. S4† and Table 1, baseline separation ($R_s \geq 1.5$) was achieved for the vast majority of racemates (20 out of 22) on column A packed with CSP-A, and high-resolution separation was achieved for several racemates, such as 4,4′-difluorobenzoin ($R_s = 9.70$), 4,4′-dimethylbenzoin ($R_s = 8.73$), methyl mandelate ($R_s = 7.82$), 4-chlorobenzhydrol ($R_s = 7.48$), and 4-methylbenzhydrol ($R_s = 7.11$), revealing the potential of CSP-A in HPLC enantioseparation. Meanwhile, CSP-B packed column B achieved baseline separation for 15 racemates (Fig. S4† and Table 1), with the best separations observed for 4,4′-difluorobenzoin ($R_s = 6.28$), 4,4′-dimethylbenzoin ($R_s = 4.56$), 2,2,2-trifluoro-1-(9-anthryl)ethanol ($R_s = 3.69$), and 3-(benzyloxy)propane-1,2-diol ($R_s = 3.64$). Evidently, 18 racemates can be enantioseparated on both column A and column B (Table 1). However, these racemates achieved higher $R_s$ on column A than on column B, except for styrene oxide. This marked separation performance disparity indicates that CSP-A has a superior chiral separation capability, likely due to the unique cationic imidazolium spacer of CSP-A. It is proposed that the cationic imidazolium moieties strengthen some interactions between the CSP-A and enantiomers, such as electrostatic and hydrophilic/hydrophobic interactions, thereby improving enantioseparation. These findings highlight the strategic advantage of incorporating charged cationic imidazolium

functional groups into the design of CSPs for enhanced chromatographic resolution.

To further highlight the advantages of the two CTSM-based columns, the separation of these racemates was also performed on two commercial HPLC columns (Chiralpak AD-H and Chiralcel OD-H) for comparison. The comparative data and chromatograms of the enantioseparations on the fabricated column A, column B, and the two commercial columns are presented in Table 1, Fig. S4 and S5.† According to Fig. S4† and Table 1, of these 26 racemates, 19 racemates can be separated on the Chiralpak AD-H column, and 19 racemates can be separated on the Chiralcel OD-H column. Meanwhile, 7 racemates cannot be separated on the Chiralpak AD-H column, and 7 racemates cannot be separated on the Chiralcel OD-H column. Among them, baseline separation of 12 racemates can be achieved on the Chiralpak AD-H column, and baseline separation of 8 racemates can be achieved on the Chiralcel OD-H column. Moreover, three racemates (3-hydroxy-2-butanone, 1-phenyl-1-pentanol, and 1-(4-fluorophenyl)ethanol) cannot be separated on either of the two commercial columns; however, baseline separation of them can be achieved on column A. In addition, the separation of some racemates on the Chiralpak AD-H and Chiralcel OD-H columns is inferior to that on column A. For example, the $R_s$ values of 1,1′-bi-2-naphthol, 4-methylbenzhydrol, 1-indanol, 1-phenyl-1-propanol, 2-phenyl-1-propanol, and styrene oxide on Chiralpak AD-H are lower
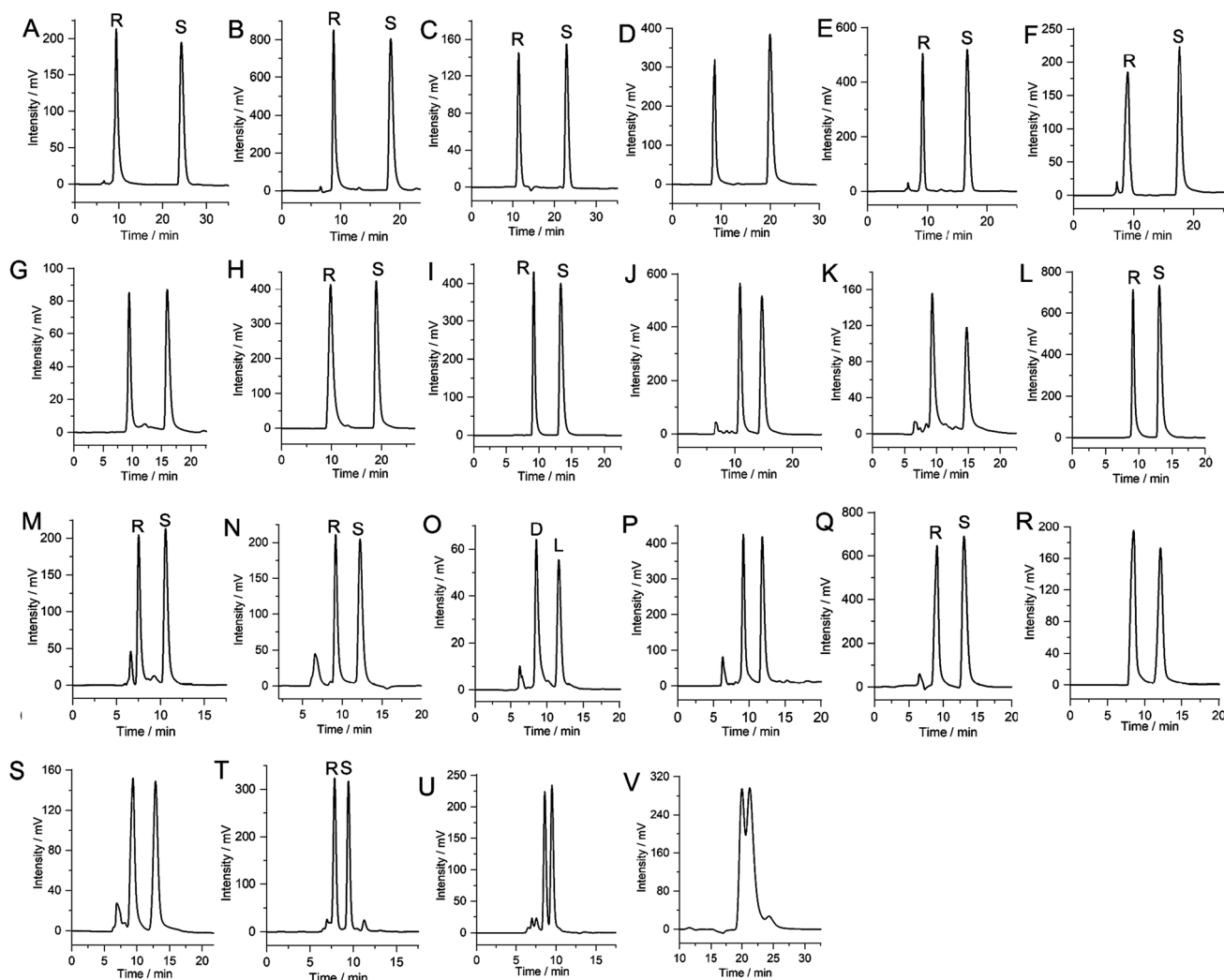
**Fig. 4** HPLC chromatograms obtained on CSP-A-packed column A. (A) 4,4′-Difluorobenzoin, (B) 4,4′-dimethylbenzoin, (C) methyl mandelate, (D) 4-chlorobenzhydrol, (E) 4-methylbenzhydrol, (F) 1,1′-bi-2-naphthol, (G) 3-hydroxy-2-butanone, (H) ethyl mandelate, (I) 1-phenylethanol, (J) 1-indanol, (K) ketoprofen, (L) 2-methoxy-2-phenylethanol, (M) 1-phenyl-1-pentanol, (N) benzoin, (O) mandelic acid, (P) 2-phenylcyclohexanone, (Q) 1-(4-fluorophenyl)ethanol, (R) 1-phenyl-1-propanol, (S) 2-phenyl-1-propanol, (T) 1-(4-fluorophenyl)ethanamine, (U) styrene oxide, and (V) amlodipine.

than those on column A. Similarly, the $R_s$ values of 4,4′-difluorobenzoin, 4-methylbenzhydrol, 1,1′-bi-2-naphthol, 1-phenylethanol, 1-indanol, 2-methoxy-2-phenylethanol, 2-phenylcyclohexanone, 1-phenyl-1-propanol, and 1-(4-fluorophenyl)ethanamine on Chiralcel OD-H are also lower than those on column A. These results show that CTSM-based column A has a good chiral recognition complementarity with the two commercial chiral columns for the separation of those tested racemates.

Comparing the separation results of the two prepared CTSM-based CSPs, both exhibit excellent enantioselectivity, which is undoubtedly attributed to the unique structure and chiral microenvironment provided by the CTSM. The CTSM was constructed by a condensation reaction of 3,3′-dihydroxy (1,1′-biphenyl)-4,4′-dicarboxaldehyde with (1R,2R)-1,2-diaminocyclohexane, forming a triangular-shaped, rigid molecule with an intrinsic cavity. Each CTSM molecule features a well-

defined cavity that can accommodate chiral guests, enabling abundant host-guest interactions. Moreover, CTSM is rich in N and O atoms in its structure. The vast majority of the separated racemates contain hydrogen bond donor groups, such as hydroxyl (–OH), carboxyl (–COOH), and amino groups (–NH₂) (Fig. S3†), which can readily form strong hydrogen bond interactions with the N and O atoms of the CTSM, indicating that the hydrogen bond interaction plays an important role in chiral resolution. Furthermore, dipole–dipole interactions also play an important role in improving enantioseparation. For example, 4,4′-difluorobenzoin and 4,4′-dimethylbenzoin, as well as 4-chlorobenzhydrol and 4-methylbenzhydrol, are structurally similar. The difference is that the substituents in 4,4′-difluorobenzoin and 4-chlorobenzhydrol are highly electronegative F and Cl, respectively, while those in 4,4′-dimethylbenzoin and 4-methylbenzhydrol are –CH₃. However, the sep-
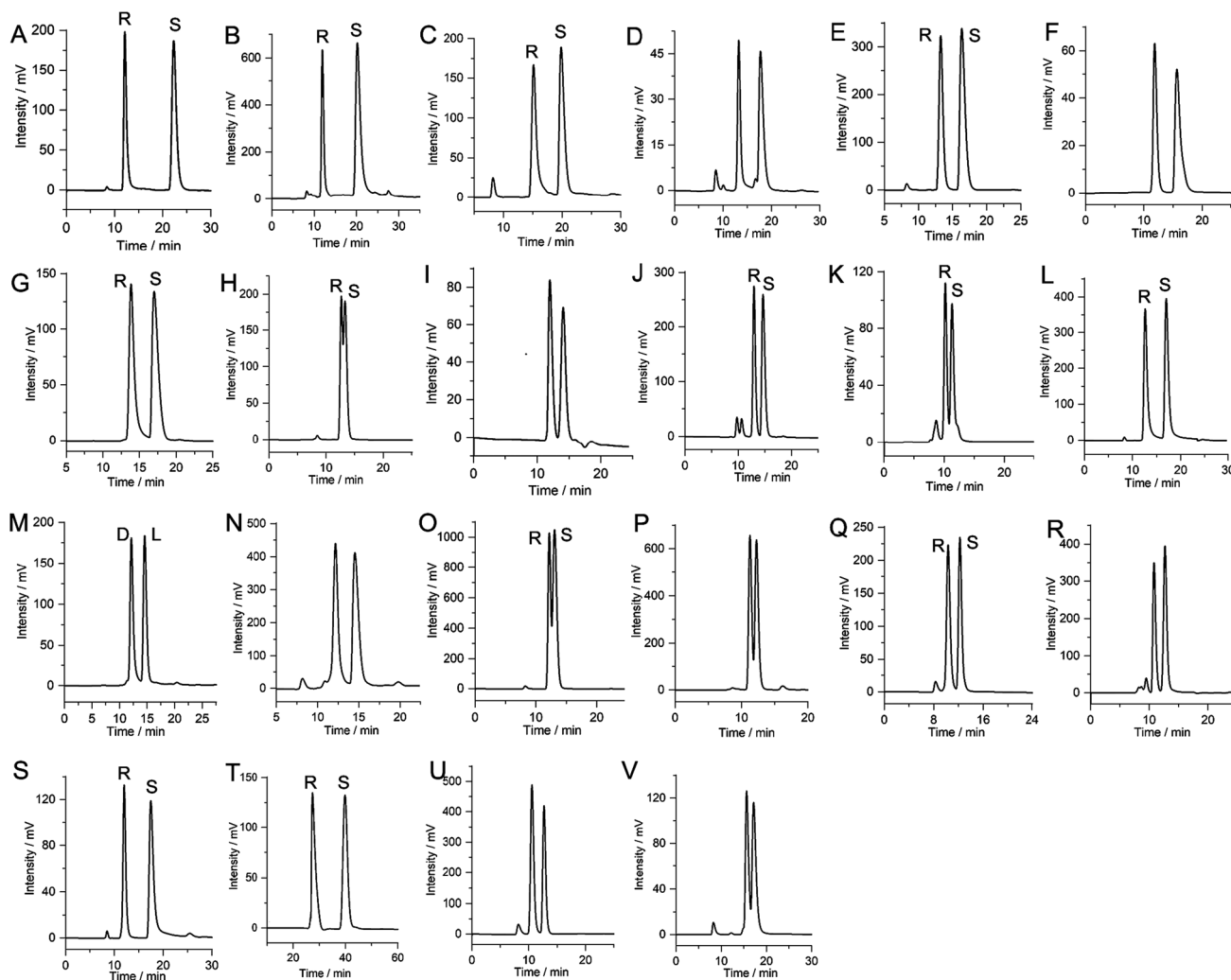
**Fig. 5** HPLC chromatograms obtained on CSP-B-packed column B. (A) 4,4′-Difluorobenzoin, (B) 4,4′-dimethylbenzoin, (C) methyl mandelate, (D) 4-chlorobenzhydrol, (E) 4-methylbenzhydrol, (F) 3-hydroxy-2-butanone, (G) ethyl mandelate, (H) 1-phenylethanol, (I) ketoprofen, (J) 2-methoxy-2-phenylethanol, (K) 1-phenyl-1-pentanol, (L) benzoin, (M) mandelic acid, (N) 2-phenylcyclohexanone, (O) 1-(4-fluorophenyl)ethanol, (P) 1-phenyl-1-propanol, (Q) 1-(4-fluorophenyl)ethanamine, (R) styrene oxide, (S) 2,2,2-trifluoro-1-(9-anthryl)ethanol, (T) 3-(benzyloxy)propane-1,2-diol, (U) 1-phenylethylamine, and (V) flavanone.

aration of 4,4′-difluorobenzoin is better than that of 4,4′-dimethylbenzoin, and the separation of 4-chlorobenzhydrol is also better than that of 4-methylbenzhydrol. This may be attributed to the stronger dipole–dipole interactions between 4,4′-difluorobenzoin and CSPs compared to those between 4′-dimethylbenzoin and CSPs, as well as the stronger dipole–dipole interactions between 4-chlorobenzhydrol and CSPs compared to those between 4-methylbenzhydrol and CSPs. Additionally, most analytes are chiral aromatic compounds, and the CTSM contains abundant benzene rings that can engage in π–π interactions with enantiomers, thus enhancing enantioseparation. It is challenging to precisely elucidate the chiral separation mechanisms between the CTSM-based CSPs and racemates, as these mechanisms involve the complex chiral microenvironment and interaction processes. Taken overall, the interactions between CSPs and enantiomers, such

as hydrogen-bonding, dipole–dipole, π–π, van der Waals force, and electrostatic interactions, play important roles during enantioseparation.

### 3.3 Effect of analyte mass

The effect of analyte mass on chiral separation using CSP-A and CSP-B packed columns was evaluated at 25 °C (Fig. 6). The injection masses of 1-phenylethanol and ethyl mandelate were increased from 1 to 20 μg, resulting in insignificant changes of the retention time and resolution for the two racemates. Moreover, the peak areas of the two enantiomers increased linearly with increasing injection masses. When the injection mass was raised to 20 μg, the chromatograms obtained from both column A and column B continued to show sharp peaks. The column loading capacities for the separations of 1-phenylethanol on column A and ethyl mandelate on column B were
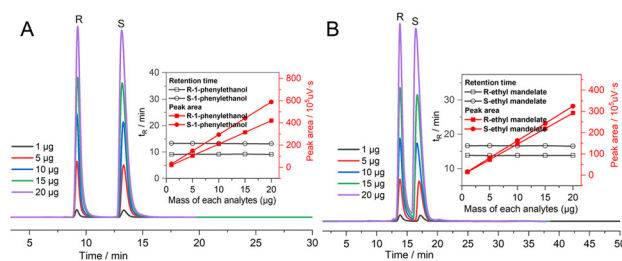
**Fig. 6** Chromatograms of analytes on the prepared columns with varying injected masses (column temperature: 25 °C; mobile phase: $n$-HEX/IPA = 90/10 (v/v); flow rate: 0.1 mL min$^{-1}$). (A) Separation of 1-phenylethanol on column A; and (B) separation of ethyl mandelate on column B.

~50 µg and ~30 µg, respectively. These results indicate that the CSP-A and CSP-B packed columns possess good column loading capacities and are suitable for analytical applications.

### 3.4 Effect of column temperature

To examine the effect of column temperature on chiral separation, 1-phenylethanol in column A and ethyl mandelate in column B were separated at different column temperatures ranging from 20 °C to 45 °C, respectively (Fig. 7). It was found that the retention time and resolution of the two racemates decreased as the column temperature increased. Moreover, the Van't Hoff plots of the enantiomers exhibited good linear correlation, suggesting that the interaction mechanism throughout the studied temperature range remained unchanged. The thermodynamic parameters were calculated and are listed in Table S2.† The negative values of $\Delta G$ for the two enantiomers indicated that the separation process on CSP-A and CSP-B is thermodynamically spontaneous, and low temperatures facilitate enantioseparation.
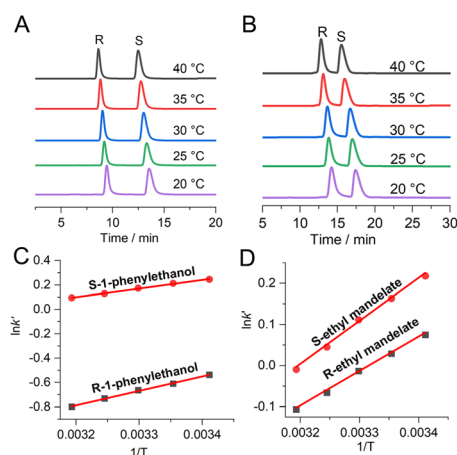


**Fig. 7** (A and C) Chromatograms and Van't Hoff plots of 1-phenylethanol on column A (column temperature: 20–40 °C; mobile phase: $n$-HEX/IPA = 90/10 (v/v); flow rate: 0.1 mL min$^{-1}$); and (B and D) chromatograms and Van't Hoff plots of ethyl mandelate on column B (column temperature: 20–40 °C; mobile phase: $n$-HEX/IPA = 90/10 (v/v); flow rate: 0.1 mL min$^{-1}$).
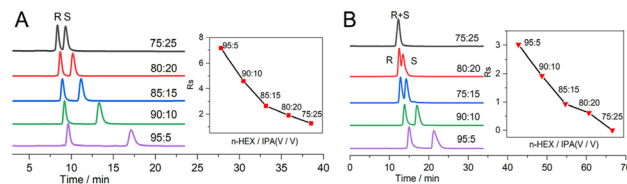


**Fig. 8** Enantioseparations of (A) 1-phenylethanol on column A and (B) ethyl mandelate on column B using different ratios of $n$-HEX/IPA as mobile phases (column temperature: 25 °C; flow rate: 0.1 mL min$^{-1}$).

### 3.5 Effect of mobile phase composition

The influence of mobile phase composition on HPLC separation of 1-phenylethanol on column A and separation of ethyl mandelate on column B was also investigated using different ratios of $n$-HEX/IPA as mobile phases. As shown in Fig. 8, with the increase of IPA, the retention time and $R_s$ for the two racemates were obviously decreased. This is most likely due to increased competition from IPA for the hydrogen bonding sites on CSPs, which weakens the hydrogen bonding interaction between CSPs and enantiomers. When a mobile phase with a low content of IPA ($n$-HEX/IPA = 95/5) is used, high-resolution separation of the two analytes is achieved, but the retention time of the enantiomers is longer. When the content of IPA is increased to 25% ($n$-HEX/IPA = 75/25), the retention time of the enantiomers is shortened, and ethyl mandelate cannot be enantioseparated, while 1-phenylethanol cannot be baseline separated. Therefore, mobile phase composition is critical for enantioseparation.

### 3.6 Reproducibility and stability

The reproducibility and stability of CSPs are quite important for their application. Therefore, separations of 1-phenylethanol and ethyl mandelate were performed on column A and column B after these columns had been reused for hundreds of injections. As shown in Fig. S6,† there were no significant changes in the retention time and $R_s$ value of the analytes after 100, 200, 300, and 400 injections compared to the original test. The relative standard deviations (RSDs, $n$ = 5) were less than 1.16% for the retention time and 3.29% for the $R_s$ value, respectively. Furthermore, to assess the column-to-column reproducibility of the two chiral columns, the separation of 1-phenylethanol was conducted on three columns packed with CSP-A (column A1, A2, and A3) prepared from different batches, and the separation of ethyl mandelate was also performed on three columns packed with CSP-B (column B1, B2, and B3) prepared from different batches. The obtained chromatograms are shown in Fig. S7,† and the RSDs ($n$ = 3) of $R_s$ and retention times were less than 8.79% and 5.04%, respectively. These results demonstrate that both chiral columns exhibit satisfactory reproducibility and stability.

## 4 Conclusions

In this study, two new HPLC CSPs with different spacers were prepared by bonding of a novel CTSM to thiol-functionalized

silica *via* a thiol-ene click strategy. The two CSPs exhibited excellent chiral separation capabilities for various racemates, including alcohols, ketones, esters, phenols, organic acids, epoxides, and amines. Because CSP-A contains a cationic imidazolium spacer in its structure, it exhibits better chiral separation performance than CSP-B. Compared to commercial Chiralpak AD-H and Chiralcel OD-H columns, the prepared CSP-A can achieve the separation of some enantiomers that cannot be separated or cannot be well separated by the two commercial columns. This work demonstrates the promising potential of CTSM for chiral separation in HPLC.

## Author contributions

Jia-Lei Wu: writing-original draft, investigation, and data curation. Hua-Can Zhang: conceptualization, software, and formal analysis. Li-Qin Yu: methodology and investigation. Sheng-Ming Xie: resources, visualization, and funding acquisition. Jun-Hui Zhang: writing-review & editing, supervision, funding acquisition, and project administration. Bang-Jin Wang: resources and funding acquisition. Li-Ming Yuan: resources, funding acquisition, and project administration.

## Data availability

The data supporting this article have been included as part of the ESI.†

## Conflicts of interest

There are no conflicts to declare.

## Acknowledgements

## References

1 G. Alvarez-Rivera, M. Bueno, D. Ballesteros-Vivas and A. Cifuentes, *TrAC, Trends Anal. Chem.*, 2020, **123**, 115761.

2 H. L. Qian, S. T. Xu and X. P. Yan, *Anal. Chem.*, 2023, **95**, 304–318.

3 B. Tang, W. Wang, H. Hou, Y. Liu, Z. Liu, L. Geng, L. Sun and A. Luo, *Chin. Chem. Lett.*, 2022, **33**, 898–902.

4 Y. Okamoto and E. Yashima, *Angew. Chem., Int. Ed.*, 1998, **37**, 1020–1043.

5 Y. Li, X. N. Jin, Y. Xiao, X. F. Ma and Y. Wang, *Analyst*, 2023, **148**, 4987–4994.

6 H. Li, K. Li, Y. Y. Cui and C. X. Yang, *Anal. Chim. Acta*, 2024, **1332**, 343377.

7 L. Bezhitashvili, A. Bardavelidze, A. Mskhiladze, M. Gumustas, S. A. Ozkan, A. Volonterio, T. Farkas and B. Chankvetadze, *J. Chromatogr. A*, 2018, **1571**, 132–139.

8 X. Lu, Y. Li, J. Yang and Y. Wang, *Chin. Chem. Lett.*, 2023, **34**, 108342.

9 C. L. Zhang, X. Y. Yu, Y. Xiao and Q. Zhang, *Analyst*, 2025, **150**, 2146–2152.

10 H. Li, X. Wang, C. Shi, L. Zhao, Z. Li and H. Qiu, *Chin. Chem. Lett.*, 2023, **34**, 107606.

11 M. H. Hyun, *J. Chromatogr. A*, 2016, **1467**, 19–32.

12 J. Y. Sung, S. M. Jin, S. Lee, S. Y. An and J. S. Jin, *Talanta*, 2021, **235**, 122739.

13 D. W. Armstrong, Y. B. Tang, S. S. Chen, Y. W. Zhou, C. Bagwill and J. R. Chen, *Anal. Chem.*, 1994, **66**, 1473–1484.

14 M. Catani, O. H. Ismail, F. Gasparrini, M. Antonelli, L. Pasti, N. Marchetti, S. Felletti and A. Cavazzini, *Analyst*, 2017, **142**, 555–566.

15 M. Lämmerhofer and W. Lindner, *J. Chromatogr. A*, 1996, **741**, 33–48.

16 J. H. Zhang, R. X. Liang, B. Huang, L. Q. Yu, J. Chen, B. J. Wang, S. M. Xie and L. M. Yuan, *Chin. Chem. Lett.*, 2025, DOI: **10.1016/j.cclet.2025.111146**.

17 J. H. Zhang, S. M. Xie and L. M. Yuan, *J. Sep. Sci.*, 2022, **45**, 51–77.

18 H. Jiang, K. W. Yang, X. X. Zhao, W. Q. Zhang, Y. Liu, J. W. Jiang and Y. Cui, *J. Am. Chem. Soc.*, 2021, **143**, 390–398.

19 J. Haginaka, C. Seyama and N. Kanasugi, *Anal. Chem.*, 1995, **67**, 2539–2547.

20 G. Sun, Y. Luo, Z. Yan, H. Qiu and W. Tang, *Chin. Chem. Lett.*, 2024, **35**, 109787.

21 T. Ogoshi, T. Yamagishi and Y. Nakamoto, *Chem. Rev.*, 2016, **116**, 7937–8002.

22 J. Murray, K. Kim, T. Ogoshi, W. Yao and B. C. Gibb, *Chem. Soc. Rev.*, 2017, **46**, 2479–2496.

23 R. Kumar, A. Sharma, H. Singh, P. Suating, H. S. Kim, K. Sunwoo, I. Shim, B. C. Gibb and J. S. Kim, *Chem. Rev.*, 2019, **119**, 9657–9721.

24 H. Li, Y. Qi, J. Chen, J. Wang, M. Yang and H. Qiu, *Chin. Chem. Lett.*, 2024, **35**, 109659.

25 G. Sun, X. Zhang, Z. Zheng, Z. Y. Zhang, M. Dong, J. L. Sessler and C. Li, *J. Am. Chem. Soc.*, 2024, **146**, 26233–26242.

26 Y. Z. Liu, H. L. Wang, L. Q. Shangguan, P. R. Liu, B. B. Shi, X. Hong and F. H. Huang, *J. Am. Chem. Soc.*, 2021, **143**, 3081–3085.

27 C. Shi, H. Li, X. Shi, L. Zhao and H. Qiu, *Chin. Chem. Lett.*, 2022, **33**, 3613–3622.

28 J. R. Wu and Y. W. Yang, *Angew. Chem., Int. Ed.*, 2021, **60**, 1690–1701.

29 C. H. Wang, L. Xu, Z. H. Jia and T. P. Loh, *Chin. Chem. Lett.*, 2024, **35**, 109075.

30 A. Radujević, A. Penavic, R. Z. Pavlović, J. D. Badjić and P. Anzenbacher, *Chem*, 2022, **8**, 2228–2244.

31 R. Pinalli, A. Pedrini and E. Dalcanale, *Chem. Soc. Rev.*, 2018, **47**, 7006–7026.

32 P. Sun, C. L. Wang, Z. S. Breitbach, Y. Zhang and D. W. Armstrong, *Anal. Chem.*, 2009, **81**, 10215–10226.

33 Y. Zhang, Z. S. Breitbach, C. L. Wang and D. W. Armstrong, *Analyst*, 2010, **135**, 1076–1083.

34 B. Huang, K. Li, Q. Y. Ma, T. X. Xiang, R. X. Liang, Y. N. Gong, B. J. Wang, J. H. Zhang, S. M. Xie and L. M. Yuan, *Anal. Chem.*, 2023, **95**, 13289–13296.

35 T. Li, H. Li, J. Chen, Y. L. Yu, S. Chen, J. H. Wang and H. D. Qiu, *J. Chromatogr. A*, 2024, **1720**, 464799.

36 T. Sun, Y. L. Song, Y. Y. Zhang, M. Y. Ba, W. Li, Z. Q. Cai, S. Q. Hu, X. M. Liu and S. S. Zhang, *Talanta*, 2024, **273**, 125877.

37 Y. Li, X. R. Yang, W. Jiang, G. P. Huang, Y. Wang and Y. Xiao, *Anal. Chem.*, 2024, **96**, 12622–12629.

38 X. M. Shuai, Z. Q. Cai, Y. J. Chen, X. Y. Zhao, Q. Q. Song, K. X. Ren, X. X. Jiang, T. Sun and S. Q. Hu, *Microchem. J.*, 2020, **157**, 105124.

39 M. Kwit, J. Grajewski, P. Skowronek, M. Zgorzelak and J. Gawroński, *Chem. Rev.*, 2019, **19**, 213–237.

40 J. Szymkowiak, B. Warżajtis, U. Rychlewska and M. Kwit, *Chem. – Eur. J.*, 2018, **24**, 6041–6046.

41 D. L. He, R. Clowes, M. A. Little, M. Liu and A. I. Cooper, *Chem. Commun.*, 2021, **57**, 6141–6144.

42 A. Dey, S. Chand, B. Maity, P. M. Bhatt, M. Ghosh, L. Cavallo, M. Eddaoudi and N. M. Khashab, *J. Am. Chem. Soc.*, 2021, **143**, 4090–4094.

43 Y. P. Zhang, K. Li, L. X. Xiong, B. J. Wang, S. M. Xie, J. H. Zhang and L. M. Yuan, *J. Chromatogr. A*, 2022, **1683**, 463551.

44 W. Inoue, K. Kazama, M. Tsuboi and M. Miyasaka, *J. Photochem. Photobiol., A*, 2022, **425**, 113688.

45 A. Dey, S. Chand, M. Ghosh, M. Altamimy, B. Maity, P. M. Bhatt, I. A. Bhat, L. Cavallo, M. Eddaoudi and N. M. Khashab, *Chem. Commun.*, 2021, **57**, 9124–9127.

46 B. Hua, Y. J. Ding, L. O. Alimi, B. Moosa, G. W. Zhang, W. S. Baslyman, J. Sessler and N. M. Khashab, *Chem. Sci.*, 2021, **12**, 12286–12291.

47 X. F. Zhu, G. W. Zhang, L. O. Alimi, B. M. Moosa, A. H. Emwas, F. Fang and N. M. Khashab, *Chem. Mater.*, 2023, **35**, 9160–9166.

48 H. C. Kolb, M. G. Finn and K. B. Sharpless, *Angew. Chem., Int. Ed.*, 2001, **40**, 2004–2021.

49 C. H. Chu and R. H. Liu, *Chem. Soc. Rev.*, 2011, **40**, 2177–2188.

50 Y. Wang, J. K. Chen, L. X. Xiong, B. J. Wang, S. M. Xie, J. H. Zhang and L. M. Yuan, *Anal. Chem.*, 2022, **94**, 4961–4969.

51 M. J. Wan, Y. C. Zheng, X. M. Dai, H. L. Yang, J. Q. Zhou, J. Ou, Y. X. Yang, M. F. Liao, Z. N. Xia and L. J. Wang, *Chem. Mater.*, 2023, **35**, 609–616.

52 M. Chen, X. L. Lu, X. F. Ma, Y. Xiao and Y. Wang, *Analyst*, 2021, **146**, 3025–3033.

53 D. L. He, H. Ji, T. Liu, M. Yang, R. Clowes, M. A. Little, M. Liu and A. I. Cooper, *J. Am. Chem. Soc.*, 2024, **146**, 17438–17445.